Recent Developments for ECR Ion Sources at HIMAC

A. Kitagawa[1)], M. Muramatsu[1)], M. Sekiguchi[1)], S. Yamada[1)], T. Okada[2)], M. Yamamoto[2)], S. Biri[3)], and K. Uno[4)]
1) National Institute of Radiological Sciences, 4-9-1 Anagawa, Inage, Chiba 263-8555, Japan,
2) Accelerator Engineering Corporation, 2-10-14 Konakadai, Inage, Chiba 263-0043, Japan,
3) Institute of Nuclear Research (ATOMKI), H-4026 Debrecen, Bem ter 18/C, Hungary,
4) Sumitomo Heavy Industry, Ltd., 5-2 Soubiraki, Niihama, Ehime 792-8588, Japan.
E-mail: kitagawa@nirs.go.jp.

Two ECR ion sources are installed for the Heavy Ion Medical Accelerator in Chiba (HIMAC) at the National Institute of Radiological Sciences (NIRS). One of them, the NIRS-ECR, is a 10GHz ECR ion source, and is mainly operated to produce C^{4+} ions for the daily clinical treatment. The other source, the NIRS-HEC, is an 18GHz ECR ion source, and is expected to produce heavier ion species. Developments for increasing the beam intensity are now in progress. In order to realize the uniform ion-density distribution at the extraction aperture for the higher beam intensity, the radial magnetic field given by the permanent sextupole magnet has been optimized. An aluminum chamber for the NIRS-HEC has been tested to increase the cold electron supply into the ECR plasma. An additional microwave-injection system with a wide frequency range of 10 to 18GHz, which allows to investigate the effects of two-frequency heating, has been installed.

I. Introduction

High-energy heavy-ion radiotherapy has two clear advantages, i.e., the good localized dose distribution and the large relative biological effectiveness[1]. HIMAC has carried out clinical trials by carbon beams with an energy of 290-400MeV/u since 1994[2]. Over 500 patients have already been treated and got good preliminary results.

HIMAC consists of three treatment rooms, a beam delivery system, two 800MeV/u synchrotron rings, a 6MeV/u Alvarez linac, and an 800keV/u RFQ linac. HIMAC is not only dedicated to cancer therapy, but also utilized with various ion species for basic experiments of biomedical science, physics, chemistry, material sciences, etc. For these requirements, three ion sources (one PIGIS and two ECRISs) are installed[3-5]. PIGIS is mainly utilized to produce ions by spattering a solid material. ECRISs are expected to produce intensive highly charged ions with easy operation and maintenance.

The history of developments of ECR ion sources at HIMAC has four major trends, (a) the optimization of the extraction configuration, (b) the electron supply, (c) the enhancement of the ECR region, and (d) the afterglow phenomenon. (a) The experimental results and the computer simulation on the extraction configuration were studied[4,6] in the NIRS-ECR. The optimization of the extraction electric field improved the transmission efficiency of the extracted beam. In addition, the NIRS-HEC shows the importance of the optimization of the radial magnetic field. It is presented in this paper. (b) The bias probe at the NIRS-ECR improved the beam intensity[4], but the operation parameters are sensitively affected by the probe condition. We finally had to abort the bias probe and take an easy operation for the daily medical use. In this paper, we report the possibility of an aluminum chamber as another trial for the electron supply. (c) In order to enhance the ECR region, we observed 14 and 18GHz two-frequency heating in the Hyper ECR at INS, Univ. of Tokyo[7]. It seemed the mixing of microwaves slightly improved the source performance. However one frequency always disturbed the others. It seems that a part of 18GHz microwave cannot penetrate through the plasma maintained by 14GHz microwave[8]. The phenomenon is too complex to understand. We desire to observe the frequency dependence of the mixing by using an additional microwave-

II. Description of the sources

A schematic view of the NIRS-HEC is shown in Fig.1. Since the RFQ linac requires heavy ions with an energy of 8keV/u and a charge-to-mass ratio larger than 1/7, each source is set on a high voltage platform with the maximum voltage of 56 kV. The NIRS-HEC has a single closed ECR zone, and the mirror axis of the source is aligned with the vertical line. The minimum B structure consists of two mirror magnet coils and a sextupole permanent magnet. The microwave and ionized gases are axially fed into a plasma chamber. The electric potentials of all components, which include the plasma chamber, the mirror magnets, the sextupole magnet, a vacuum chamber and pumps, and all power supplies, are equivalent as the high voltage platform. The negative extraction voltage is applied to an extraction electrode against the high voltage platform. An insulator is only used between the extraction electrode and the vacuum chamber, and has enough electric resistance. Since the proof of the high voltage is only determined by the vacuum pressure at the extraction region, the maximum extraction voltage reaches at 60kV. The beam is vertically extracted, and is analyzed by a 90 degree bending magnet. The mirror coils and the vacuum chamber are vertically rifted up to remove the plasma chamber for the maintenance. Other details are shown in Table I.

A schematic view of the NIRS-ECR is shown in Fig.2. Other details are also shown in Table I.

The performance for various gaseous ions has been measured. Typical output currents of both sources are shown in Table II. Natural gases are used for the production of ^{84}Kr, and ^{132}Xe, and the MIVOC technique[9] is used for Fe.

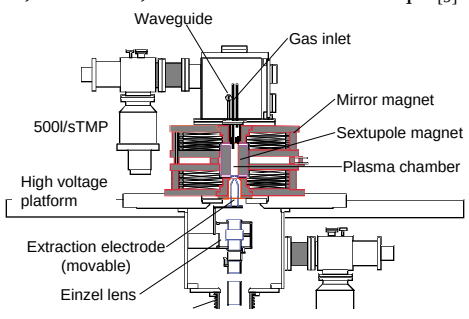

Fig.1 Schematic view of the NIRS-HEC.

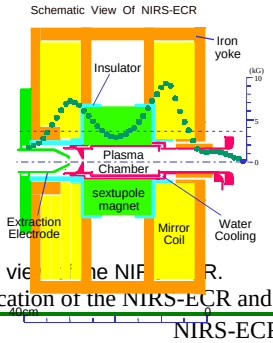

Fig.2 Schematic vie[illegible]e NIR[illegible]R.

Table I. Specification of the NIRS-ECR and the NIRS-HEC

	NIRS-ECR	NIRS-HEC	
Solenoid			
Yoke outer length	358	410	mm
Yoke outer diameter	650	730	mm
Maximum current	600/600	800/800	A
Maximum field on axis	9.3/7.2	12.2/12.2	kG
Typical mirror ratio	3.1/2.4	2.2	
Sextupole			
Material	NdFeB	NdFeB	
Length	150	200	mm
Inner diameter	76	66	mm
Field on magnet surface	9	14	kG
Plasma chamber			
Material	Cu	Cu or Al	
Chamber inner diameter	70	61	mm
Gas-injection port #	quartz & SUS tube	quartz & SUS tube	
Vacuum pressure without gas	$1x10^{-7}$	$6x10^{-8}$	torr
Microwave			
Frequency	10	18	GHz
Maximum power	1.8	1.2	kW
Operation mode	CW/pulse	CW/pulse	
Injection	waveguide direct	waveguide direct	
Extraction			
Structure	single gap	single gap	
Maximum voltage	25	60	kV
Diameter of aperture	13	10 or 12	mm
Extraction gap	15-60	15-90	mm
Focusing element	Einzel & Solenoid	Einzel	

Table II. Records of beam intensities of NIRS-ECR and NIRS-HEC. The NIRS-HEC is shown in bold face. Currents are in eμA.

q+	He	C	N	O	Ne	Ar	Fe	^{84}Kr	^{132}Xe
1+	3200 **4000**								
2+	2100	470	790	660	622				
3+			590	590	700 **650**				
4+		430	340	440	680 **600**	410			
5+		(50)	220	280	600 **320**	345			
6+			25	130	220 **100**	365 **320**			
7+				15	54	300 **400**			
8+					10	300 **800**	**35**	160	
9+					0.6	105 **400**	**60**	125	
11+						7 **70**	**40**	55 **90**	15
12+						**10**	**30**	30	11
13+						**4**	**15**	20 **140**	10
14+									7
15+								**60**	
16+									4
20+									**45**
21+									**30**

III. Developments

A. Optimization of the radial magnetic field

The experimental results on the NIRS-HEC show that the extracted beam intensity is strongly affected by the cross sectional ion-density distribution and the extraction electric field at the extraction aperture[5,10]. The real ion-density distribution cannot be observed, however we assumed the highly charged ions are localized inside of the ECR zone and the ion trajectory from the ECR zone to the extraction aperture is tightly bound the magnetic flux line. Therefore the ion-density distribution depends on the magnetic trap configuration. The ion-density distribution of the previous NIRS-HEC is shown in Fig.3. It is estimated by the modified TrapCAD code[11] which calculates the magnetic flux density n. Only the magnetic flux lines running through the ECR surface are taken into account to evaluate n. Since the narrow concentrated ion-density distribution at the extraction slit like Fig.3 enhances the space charge effects, the extracted beam intensity is lower in this case than in the case with a uniform distribution. The inner diameter of the sextupole magnet in the case of the previous NIRS-HEC was designed very compact to keep a strong magnetic confinement. However it caused the strong concentration of the flux.

In order to realize the uniform ion-density distribution at the extraction aperture for the higher beam intensity, the radial magnetic field given by the permanent sextupole magnet has been optimized. The diameter of the ECR zone determined by the inner diameter of the sextupole magnet was enlarged, and consequently by the density of the flux

Fig. 3 Calculated flux-density distribution at the extraction slit.

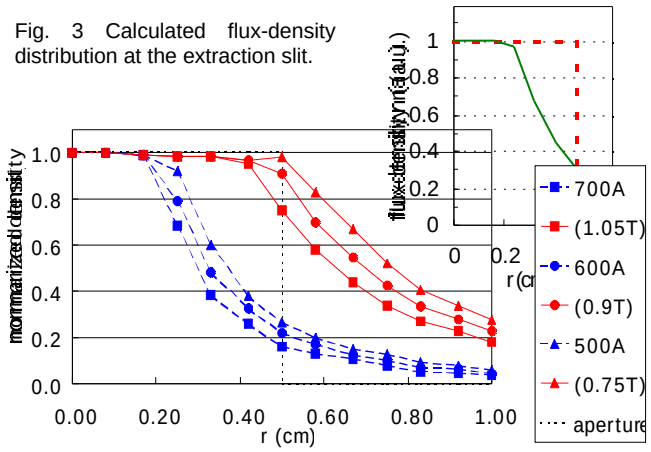

Fig.4 Flux-density distributions of the previous (broken li and present (solid lines) sextupole magnets with various mirror magnetic fields.

lines running through the ECR zone decreased at the

at various inner diameters of the sextupole magnet. The present ion-density distribution, which is indicated by solid lines, could become more uniform.

The inner diameter of the sextupole magnet was increased from 46mm to 66mm, so that the extracted intensities of Ar^{8+} and Ar^{9+} ions increased from 250 and 150 eμA up to 800 and 400 eμA, respectively.

The NIRS-ECR is also under modification to optimize the radial magnetic field. The new sextupole magnet will be replaced by this summer.

B. Effectiveness of the aluminum chamber wall

The importance of the cold electron supply into the plasma for the production of highly charged ions has been pointed out by many groups[12-16]. The wall coating is one of most convenient technique for the improvement of the beam intensity. An aluminum chamber which wall surface was naturally covered with the aluminum oxide layer was tested. The new aluminum chamber has a same size and structure as the previous copper one.

Fig.5 shows the typical charge state distributions for Ar ions produced with the copper and aluminum chamber. In the case of the aluminum chamber, the charge state distribution has been shifted to the lower charge. We couldn't find the optimized parameter for highly charged ions. It shows different results as compared with well-known situations in other ion sources. We have continued the tests under more various conditions, and try to compare with effects by other cold electron suppliers. A movable bias probe has been installed at the NIRS-HEC.

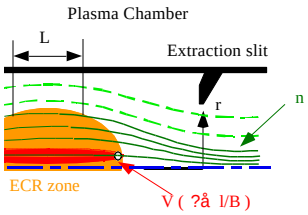

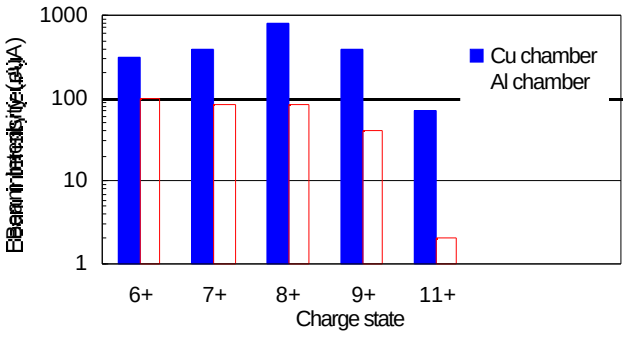

Fig.5 Typical charge distributions for Ar ions with the aluminum and copper chamber.

C. Additional microwave-injection system with a wide frequency range for the two-frequency heating

The relation between the volume of the ECR region and the source performance has been not verified. However several reports pointed out the possibility of improvement by the increasing the amount of the ECR region, i.e., 2ω mode[17], also have tested the two-frequency heating.

In order to investigate the effects of two-frequency heating, an additional microwave-injection system with a wide frequency range of 10 to 18GHz was developed. Fig.6 shows a schematic view of the system. A synthesizer can generate and modulate any amplitudes and frequencies between 10 and 18GHz. A TWT amplifier also has a sufficient gain in such a frequency range, and has a maximum power of 250W. All components, straight and bending wave guides, an arc sensor, a power monitor, and a vacuum window, have the double-ridge wave guide structure, and its frequency range is also verified. From the measurement of VSWR between 10 and 18GHz, the total reflection power of the system is less than 3%. In addition, the power monitor as the feedback loop keeps to stabilize the forward power in all frequency range.

The TrapCAD code can calculate the electron acceleration process with two resonance frequencies in the base of a single particle motion of electron. We expect that the frequency dependence of the experimental ion charge state distributions and the simulated electron energy distributions gives us useful knowledge on the relation between the plasma volume and the source performance. The first plasma with this system has been observed.

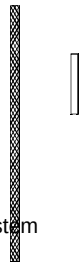

Fig. 6 Microwave-injection system with a wide frequency range.

IV. Conclusion

Some developments on the beam extraction configuration, the electron supply, and the enhancement of the ECR region, has been tested. The optimization of the radial magnetic field gave us most evident improvement of the source performance. The typical output currents for the various ion species increased by twice or four times. Fe, Kr and Xe ions have been supplied to synchrotron users successfully. On the other hand, the aluminum chamber shifted the charge state distribution to lower charge. It is an opposite effect as the desired one. Other trials are now in progress.

Acknowledgment

The authors thank Prof. T. Hattori (Tokyo Institute of Technology) and Prof. Liu (IMP, Lanzhou) for suggestions on the design study and development, and Prof. Y. Kato (Toyama Pref. Univ.) and Prof. Y. Yoshida (Yamanashi Univ.) for discussions on the plasma. The current research was partly supported by a Hungarian-Japanese intergovernmental scientific-technological co-operation between the National Technical Development Committee (OMFB) and the Science and Technology Agency (STA). Reference number: OMFB-TET-J-6/98.

References

[1] *Biological and Medical Research with Accelerated Heavy Ions at the Bevalac*, LBL-11220, UC-48(1980)

[4] A. Kitagawa *et al.*, Rev. Sci. Instrum, **65**(1994)1087.
[5] A. Kitagawa *et al.*, Rev. Sci. Instrum, **69**(1998)674.
[6] S. Fu *et al.*, Rev. Sci. Instrum, **65**(1994)1435.
[7] Y. Yamashita *et al.*, *Proc. of the 12th Intnl. Workshop on ECRIS*, Wako, INS-J-182, 1995, p.289.
[8] R. Geller, *Proc. of the 11th Intnl. Workshop on ECRIS*, Groningen, KVI-Report 996, 1993, p.1.
[9] J. Arje *et al.*, *Proc. of the 12th Intnl. Workshop on ECRIS*, Wako, INS-J-182, 1995, p.136.
[10] M. Yamamoto *et al*., *Proc. of the 11th Symp. on Accelerator Sci. and Technol.*, Harima, 1997, p.171.
[11] J. Vamosi and S. Biri, Comp. Phys. Comm., **98**(1996)215
[12] C. M. Lyneis, *Proc. of the Intnl. Conf. on ECRIS and their Applications*, East Lansing, NSCL #MSUCP-47, 1987, p.42.
[13] Z. Q. Xie *et al.*, Rev. Sci. Instrum, **62**(1991)775.
[14] G. Melin *et al.*, *Proc. of the 10th Intnl. Workshop on ECRIS*, Knoxville, ORLN CONF-9011136, 1990, p.1.
[15] S. Gammino *et al.*, Rev. Sci. Instrum, **63**(1992)2872.
[16] T. Nakagawa *et al.*, Jpn. J. Appl. Phys., **31**(1992)1129.
[17] B. Jacquot and R. Geller, *Proc. of the Intnl. Conf. on ECRIS and their Applications*, East Lansing, NSCL #MSUCP-47, 1987, p.254.
[18] G. D. Alton and D.N. Smithe, Rev. Sci. Instrum, **65**(1994)775.
[19] Z. Q. Xie and C. M. Lyneis, *Proc. of the 12th Intnl. Workshop on ECRIS*, Wako, INS-J-182, 1995, p.24.